

Coriolis forces influence the secondary circulation of gravity currents flowing in large-scale sinuous submarine channel systems

Remo Cossu¹ and Mathew G. Wells²

Received 11 June 2010; revised 8 July 2010; accepted 4 August 2010; published 11 September 2010.

[1] A combination of centrifugal and Coriolis forces drive the secondary circulation of turbidity currents in sinuous channels, and hence determine where erosion and deposition of sediment occur. Using laboratory experiments we show that when centrifugal forces dominate, the density interface shows a superelevation at the outside of a channel bend. However when Coriolis forces dominate, the interface is always deflected to the right (in the Northern Hemisphere) for both left and right turning bends. The relative importance of either centrifugal or Coriolis forces can be described in terms of a Rossby number defined as $Ro = U/fR$, where U is the mean downstream velocity, f the Coriolis parameter and R the radius of curvature of the channel bend. Channels with larger bends at high latitudes have $|Ro| < 1$ and are dominated by Coriolis forces, whereas smaller, tighter bends at low latitudes have $|Ro| \gg 1$ and are dominated by centrifugal forces. **Citation:** Cossu, R., and M. G. Wells (2010), Coriolis forces influence the secondary circulation of gravity currents flowing in large-scale sinuous submarine channel systems, *Geophys. Res. Lett.*, 37, L17603, doi:10.1029/2010GL044296.

1. Introduction

[2] Sinuous submarine channels are the main conduits by which turbidity currents transport sediments to the deep ocean basins [Meiburg and Kneller, 2010]. Recent non-rotating experiments on channelized turbidity currents have shown that the morphological evolution and associated depositional histories of submarine channel systems are highly influenced by the secondary flow structures within the channel, which determine where erosion and deposition will occur [Keevil *et al.*, 2006; Straub *et al.*, 2008; Islam and Imran, 2008]. The main focus in these non-rotating experiments has been to investigate the secondary circulation due to an imbalance of centrifugal and pressure gradient forces in channel bends, which plays a major role in the formation of superelevation of levee systems at the outer bend [e.g., Straub *et al.*, 2008; Kane *et al.*, 2010]. The circulation in such a curved channel is shown in Figure 1a. At the level of the downstream velocity maximum the centrifugal forces are at a maximum. The velocity maximum usually occurs relatively close to the

base of the gravity current due to drag induced by mixing processes at the upper interface [Turner, 1973; Meiburg and Kneller, 2010]. For such velocity profiles [e.g., Corney *et al.*, 2008; Keevil *et al.*, 2006] the secondary flow near the base is directed towards the outer bend, with a return flow near the surface, in contrast to river flows. In some experiments using square channels there is an additional secondary flow directed towards the outside bend below the velocity maximum [Imran *et al.*, 2007; Islam and Imran, 2008].

[3] Coriolis forces deflect the bulk of a gravity current to the right (in the Northern Hemisphere) [Davies *et al.*, 2006; Wells, 2009], which causes a lateral tilt of the interface in a confined, straight channel. This tilt (and any secondary circulation) means that overbanking sediment flows are more likely to occur on the right hand side of the channel (looking downstream) for mid- and high latitude systems in the Northern Hemisphere, leading to an asymmetry between levee bank heights [Menard, 1955; Komar, 1969]. Observations at higher latitudes have found that the right hand side channel levee is consistently higher in the Northern Hemisphere [Klaucke *et al.*, 1997] while the left hand side channel levee is higher in the Southern Hemisphere [Carter and Carter, 1988; Bruhn and Walker, 1997]. In addition, Coriolis forces generate Ekman boundary layers in gravity currents [Wählin, 2004] as illustrated in Figures 1b and 1c, for the case of the Northern and Southern Hemisphere respectively. In previous theoretical and experimental studies by Wählin [2004] and Cossu *et al.* [2010] these boundary layers were shown to play a critical role in determining the sense of the rotationally controlled secondary circulation in gravity currents flowing down straight channels. These secondary circulations dominated by Ekman boundary layer dynamics are also observed in oceanic gravity currents [Johnson and Sanford, 1992].

[4] There are few direct observations of the velocity structure within turbidity currents because their infrequent occurrence; the great water depths and high current velocities make measurements difficult to obtain [Xu *et al.*, 2004; Meiburg and Kneller, 2010]. The dynamics of large-scale non-depositional turbidity currents are often assumed to be similar to gravity currents, so that previous experiments in sinuous channels [e.g., Keevil *et al.*, 2006; Imran *et al.*, 2007; Islam and Imran, 2008] have used studies of saline gravity currents to gain insight into the secondary circulation in turbidity currents. An open question is whether the secondary circulation in large-scale turbidity currents flowing down a sinuous channel will be dominated by centrifugal forces or by Coriolis forces. We will address this question through the use of analog laboratory experiments mounted on a rotating platform that can produce Coriolis forces. In particular we

¹Department of Geology, University of Toronto, Toronto, Ontario, Canada.

²Department of Physical and Environmental Sciences, University of Toronto, Toronto, Ontario, Canada.

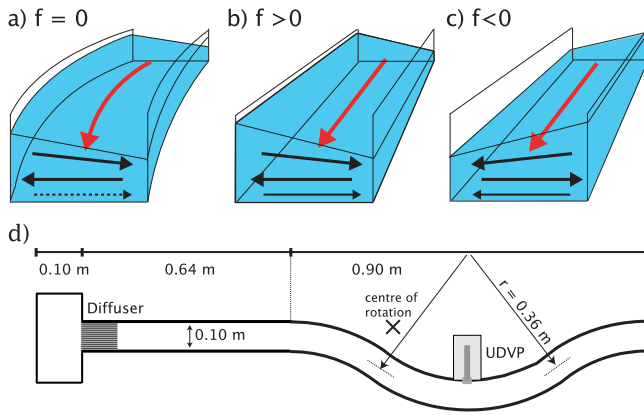


Figure 1. (a) In a curved channel the velocity maximum of the gravity current is close to the base of the flow, the secondary circulation consists of a basal flow towards the outer bend and a return flow near the surface and sometimes below the velocity maxima [Keevil *et al.*, 2006; Islam and Imran, 2008]. (b) In a straight channel Coriolis forces deflect the upper density interface and drive secondary circulations due to the presence of Ekman boundary layers. In the Northern Hemisphere ($f > 0$) the interface is deflected to the right hand side of the channel, when looking downstream, whereas (c) in the Southern Hemisphere ($f < 0$) the interface is deflected to the left hand side and the secondary circulation is in the opposite sense. Our experiment consists of (d) a curved channel that can be rotated in either the Northern or Southern Hemisphere sense.

will investigate how interface slope and the secondary circulation cells in a saline gravity current change in terms of a dimensionless Rossby number, and so determine when the flows are dominated by Coriolis or centrifugal forces.

2. Theory

[5] The geological observations of levee height asymmetry are usually described in terms of the cross-channel tilt (dh/dy) of the upper interface of the turbidity current, using the theory of Komar [1969]. Assuming that tangential friction is small and turbulence is absent, the momentum balance across the channel can then be written as

$$g' \frac{dh}{dy} = fU + \frac{U^2}{R}, \quad (1)$$

where U is the mean downstream velocity, R is the radius of curvature of the channel and f the Coriolis parameter, defined as $f = 2\Omega \sin \theta$, with Ω the Earth's rotation rate and θ the latitude. R is defined as positive when the bend is to the left (looking downstream), so that the force is in the same direction as the Coriolis force in the Northern Hemisphere, while turns to the right will have negative R . The Coriolis parameter f is positive in the Northern Hemisphere and negative in the Southern Hemisphere, so that the sign of dh/dy depends upon both the latitude and the curvature of the channel. The reduced gravity is $g' = g(\rho_2 - \rho_1)/\rho_1$, where the gravity current has the density ρ_2 and ρ_1 is the ambient

density of the seawater. Equation (1) can be re-arranged to give an equation for the interface slope whereby

$$\frac{dh}{dy} = Fr^2 \left(\frac{fh}{U} + \frac{h}{R} \right), \quad \text{where } Fr^2 = \frac{U^2}{g'h}. \quad (2)$$

Hence if the flow velocity remains constant, the interface deflection due to the Coriolis forces increases with latitude. We note that (2) has never been previously tested in a rotating experiment with a channel bend. The interface of the gravity current will be flat ($dh/dy = 0$) when Coriolis forces and centrifugal forces balance, which occurs when $fh/U = -h/R$ for a bend to the right in the Northern Hemisphere. This condition can be re-written in terms of a Rossby number defined as

$$Ro \equiv \frac{U}{fR} = -1. \quad (3)$$

We hypothesize that in sinuous flows with $|Ro| \gg 1$, the interface always slopes in towards the inner bend, while flows with $|Ro| \ll 1$ the interface will always slope to the right-hand-side (left-hand-side) in the Northern Hemisphere (Southern Hemisphere). We note that a complete description of the flow dynamics around a bend would require a full momentum budget including cross-stream frictional influences and non-local adjustment terms as discussed by Nidzieko *et al.* [2009]. However, we focus on (1) to (3) and point to future work that has to incorporate these features in a more thorough mathematical model.

3. Experiments

[6] All experiments were conducted in a channel placed within a $1.85 \text{ m} \times 1.0 \text{ m} \times 0.35 \text{ m}$ rectangular tank. This tank was rotated at a constant rate, with Coriolis parameters from $f = 0$ to $\pm 0.5 \text{ rad s}^{-1}$. Before the experiment began, the tank had to be spun up for at least 30 min in order to achieve solid body rotation of the water. The channel had a constant, rectangular cross-section with a width of 10 cm and a height of 8 cm (similar in dimensions to Keevil *et al.* [2006]) and was submerged by 0.1 m of water at the inflow point. As shown in Figure 1d, the channel consisted of a straight section of length 0.64 m, joined to a single channel bend of length of 0.9 m and with mean radius of $R = +0.36 \text{ m}$ (representing a sinuosity of 1.09). A constant velocity of the inflow was achieved by using a 0.10 m thick diffuser. We used a saline gravity current as an analog to a turbidity current. To visualize the slope of the gravity current interface at the bend apex, fluorescein dye was added to the saline mixture and the flow was illuminated by a thin sheet of light. The down-stream and across-stream velocity data were recorded in the apex of the left-turning channel bend using a Metflow Ultrasonic Doppler Velocity Profiler (UDVP), as used by Keevil *et al.* [2006]. Each UDVP probe records simultaneous single component velocity data along a profile of 128 points along the beam axis, at a frequency of 4 Hz. Measurement time per profile was 11 ms, with a 15 ms delay between the recording of each profile. Vertical velocity profiles were obtained from an array of 6 transducers at heights of 0.5, 1.5, 2.5, 3.5, 4.5 and 5.5 cm above the bottom. The velocities were averaged over an interval of

Table 1. Experimental Conditions^a

Parameter	Unit	Value
Reduced gravity g'	m s^{-2}	0.0981
Fluid temperature	$^{\circ}\text{C}$	5–6
Slope	-	01:50
Channel width - height - radius	m	0.1 – 0.08 – 0.36
Sinuosity	-	1.09
Flow rate Q	L s^{-1}	0.26
Duration of density currents	s	120
Depth averaged velocity U_m	m s^{-1}	0.035–0.048
Mean flow thickness h	m	0.05
Froude number $Fr = U_m/(g'h)^{1/2}$	-	0.58 ± 0.2
Flow Reynolds number $Re = U_m h/\nu$	-	$2\text{--}3.3 \times 10^3$

^aThe flow thickness h was estimated visually at the point upstream of the channel bend, and is a good estimate of the centerline depth as shown in Figure 2.

approximately 30 s after the head of the current had passed the instrument. Experimental conditions are summarized in Table 1.

4. Results and Discussion

[7] The strong dependence of the cross-stream slope of the density interface in the channel bend to changes in the Coriolis force is shown in a series of photographs in Figure 2 for various Coriolis parameter f . For $f = 0 \text{ rad s}^{-1}$, the Rossby number is infinite and the density interface slopes up towards the outer bend due to the centrifugal acceleration (Figure 2a). Such a superelevation is characteristic for non-rotating density currents in channel bends as described by *Keevil et al.* [2006] and *Straub et al.* [2008]. For a positive Coriolis parameter $f = +0.25 \text{ rad s}^{-1}$, the Rossby number is +0.55 and the tilt of the interface towards the outer bend increases as now the Coriolis and centrifugal forces act in

the same direction (Figure 2b). The experiment shown in Figure 2c has a negative Coriolis parameter $f = -0.25 \text{ rad s}^{-1}$ so that the Rossby number is -0.42 , and the Coriolis force acts in opposition to the centrifugal force and the superelevation at the outer bend of the interface is largely reduced. As the Rossby number is close to $Ro = -1$ there is an almost horizontal interface in the bend apex. For a larger negative Coriolis parameter $f = -0.5 \text{ rad s}^{-1}$ with $Ro = -0.2$, the current shown in Figure 2d now ramps up towards the inner bend and is completely reversed compared to Figure 2a. The observations in Figure 2 are typical of the approximately 100 experiments conducted using a range of g' and f . In particular the horizontal interface observed in Figure 2c is always seen when $0.35 < Ro < 0.45$ in other experiments using different g' and f .

[8] The resulting secondary circulation patterns are presented in Figure 3 for different Coriolis parameter f . In the non-rotating experiment with $f = 0 \text{ rad s}^{-1}$ the cross-stream velocity structure is broadly similar to experiments of *Keevil et al.* [2006]. Near the base of the gravity current (between 1 and 2.5 cm) the flow is directed from the inside to the outside of the bend (in the region near the inside bend) while above this flow the fluid moves from the outside towards the inside bend which causes an upwelling close to the outside. The downstream flow velocity maximum occurs at depths between $d = 1\text{--}2 \text{ cm}$. The total depth of the gravity current is $h = 5 \text{ cm}$, so that the ratio of $d/h = 0.2\text{--}0.4$. In non-rotating gravity currents, the secondary circulation pattern is determined by the position of the velocity maxima [*Corney et al.*, 2008], so that when the velocity maximum is near the base (i.e. $d/h < 0.4$), there is a flow towards the outer bend at intermediate depths, as seen in Figure 3a. Very close to the bottom at 0.5 cm there is another flow directed toward the inner bend. This thin bottom boundary flow occurred below

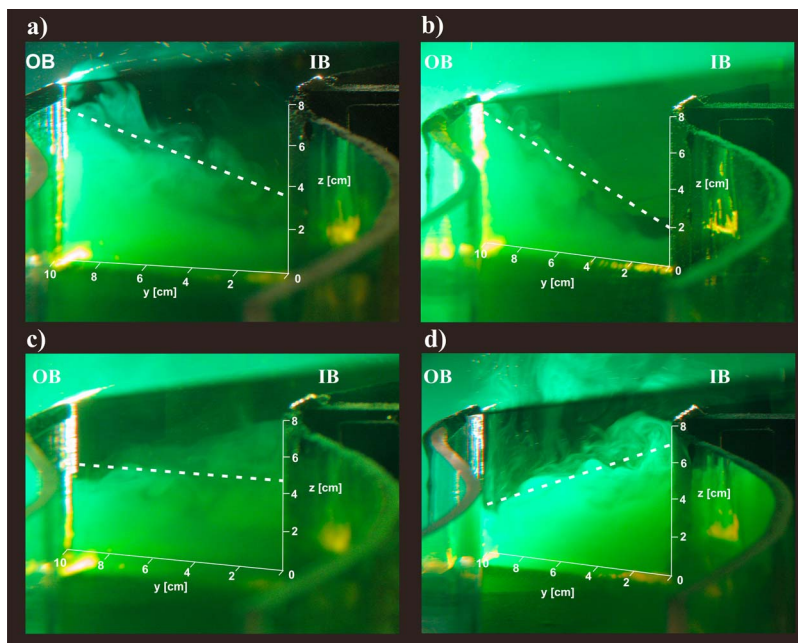


Figure 2. The photographs of the tilting interface of the gravity current are taken looking upstream at the apex of the bend. The inner and outer bends are marked as IB and OB respectively and the channel is 10 cm wide. In (a) $f = 0 \text{ rad s}^{-1}$ and the Rossby number is infinite, in (b) $f = +0.25 \text{ rad s}^{-1}$ giving $Ro = +0.55$, in (c) $f = -0.25 \text{ rad s}^{-1}$ giving $Ro = -0.42$ and in (d) $f = -0.5 \text{ rad s}^{-1}$ giving $Ro = -0.2$.

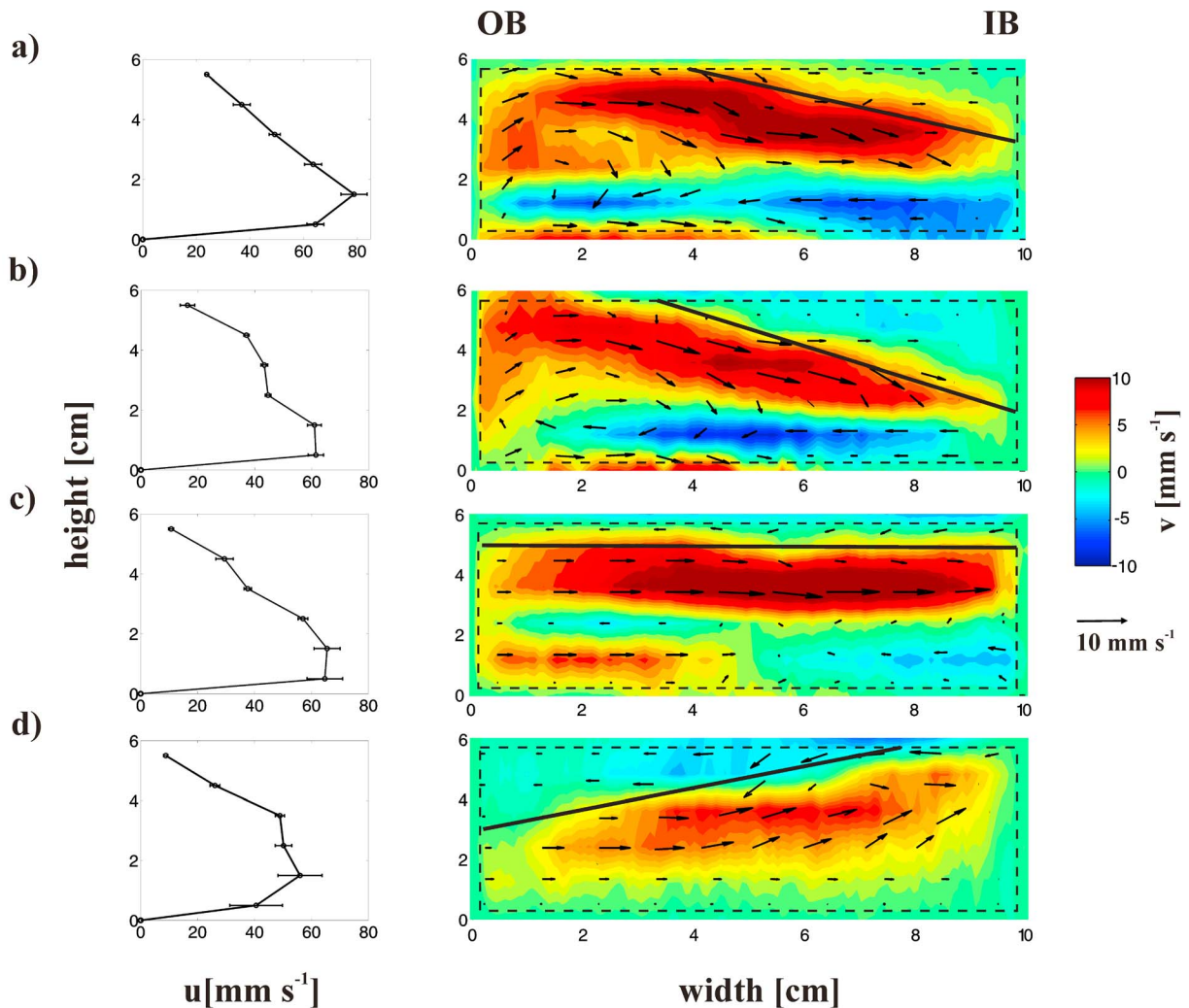


Figure 3. (left) The centreline downstream velocity profiles (u). (right) Cross-stream velocity field at the bend apex, with the contoured colours representing the v component. The dashed boundary represents the spatial extent of the UDVP measurements, and the straight line represents the interface profiles from Figure 2. The Coriolis parameter is (a) $f = 0$ rad s⁻¹, (b) $f = +0.25$ rad s⁻¹, (c) $f = -0.25$ rad s⁻¹, and (d) $f = -0.5$ rad s⁻¹.

the downstream flow maximum and is essentially the same feature observed by *Imran et al.* [2007] using a similar rectangular channel cross section. For a positive Coriolis parameter $f = +0.25$ rad s⁻¹ (Figure 3b) the corresponding flow field has a similar structure to the non-rotating experiment. However, as the centrifugal and Coriolis forces act together the tangential and upwelling velocities are intensified as is the superelevation (Figure 2b) at the outer bend.

[9] The flow pattern changes dramatically if the Coriolis parameter is negative and hence Coriolis force counteracts the centrifugal force, as seen in Figures 3c and 3d for $f = -0.25$ and -0.5 rad s⁻¹ ($Ro = 0.42$ and 0.2 respectively). In both cases, the flow towards the outside bend at mid-depth has decreased significantly compared to Figure 3a, but there is still a flow between heights of 3 to 5 cm directed toward the inner bend. The vertical flows are now almost absent in the current, suggesting that there is non-local adjustment of the velocity occurring in the downstream direction. In both Figures 3c and 3d the basal flow towards the outer bend is almost absent, suggesting that the opposition of Coriolis and

centrifugal forces suppresses this feature in rotating currents in left-turning channel bends in the Northern Hemisphere. This is in contrast to the case when the Coriolis force acts in concert with the centrifugal force, and the basal flow increased (Figure 3b). Thus only when $|Ro| \ll 1$ in a sinuous channel would there be a strong asymmetry in secondary circulation patterns between successive left and right turning channel bends.

[10] In previous studies [*Keevil et al.*, 2006; *Imran et al.*, 2007; *Straub et al.*, 2008] secondary flows were reported to be of order of 10% of the mean flow. For our rotating experiments we find similar values with the secondary flows being between 5–15 mm s⁻¹, which is about 10–20% of the mean downstream velocity. As sketched in Figure 1b the currents in Figure 3 will have Ekman boundary layer flows directed towards the inner bend for positive f . For a value of $f = +0.25$ rad s⁻¹ the Ekman number ($Ek = \nu/fH^2$) is one for a thickness of $H = 0.2$ cm, suggesting the Ekman boundary layer is much less than 1 cm in our experiments and hence may not be detectable with the UDVP in

Figure 3. Despite being unable to explicitly resolve these thin boundary layers at large f , these Ekman flows are central to driving the significant cross-stream flows we report in the present paper.

[11] The importance of the Coriolis force on gravity current dynamics becomes evident when we compare the Amazon submarine channel, located at latitudes between 3° – 7° , with the North Atlantic Mid-Ocean channel (NAMOC) located at latitudes of 53° – 59° . The low latitude Amazon submarine channel system exhibits a strong sinuosity over several hundred kilometers and consistently has the highest levee banks on the outside of channel bends. Pirmez and Imran [2003] reported a mean radius of curvature of between 1–2 km and estimated mean streamwise velocities of turbidity currents between 1 – 3 m s $^{-1}$. The Coriolis parameter for this range of latitudes is between $f = 0.076 - 0.177 \times 10^{-4}$ rad s $^{-1}$ so that the magnitude of the Rossby number for the submarine channel system is approximately between 30–130, i.e. $|Ro| \gg 1$. These large Rossby numbers indicate that Coriolis forces are negligible and the flow dynamics in the channel bends are dominated by centrifugal forces. Hence, the superelevation is on the outside bend and the resulting secondary flow field promotes upwelling at the outside (like in Figure 3a), leading to the levee asymmetry between inner and outer bends.

[12] By way of contrast the NAMOC channel has low sinuosity with observations [Klaucke et al., 1997] suggesting that the mean radius of curvature of the channel is mostly 10–20 km and the predicted mean velocity is in the range 0.2–1 m s $^{-1}$. At latitudes between 53° – 59° N the Coriolis parameter is an order of magnitude larger at $f = 1.16 - 1.2 \times 10^{-4}$ rad s $^{-1}$ so that the resulting Rossby number is between 0.05–0.5, with an average value of 0.2, i.e. $|Ro| \ll 1$. The NAMOC channel system shows a continuous higher right levee system irrespective of left or right turning bends [Klaucke et al., 1997] consistent with Coriolis force rather than centrifugal forces dominating the secondary circulation and movement of sediment within the channel. Figures 2 and 3 clearly demonstrate that the Coriolis forces are important for high latitude submarine channel systems and give rise to flow patterns that explain the observations of levee height asymmetry in these channel systems.

5. Conclusions

[13] The influence of Coriolis forces upon the flow dynamics that we have reported in this paper will have implications for the nature of depositional units such as the “outer-bank bars” (OBB) or “point bars”, as the orientation of secondary flows affects the position and geometry of these deposits [Peakall et al., 2007; Amos et al., 2010]. The outer-bank bars are depositional units that are likely to be sand prone and hence of high porosity which has significant implications for prediction of hydrocarbon reservoirs [Nakajima et al., 2009]. Based upon the data in Figures 2 and 3 we predict that Coriolis forces will affect the secondary circulation in successive bends of a sinuous channel differently; directing flow first towards the outer bank and then to the inner bank then back to the outer, as the channel turns to the left then to the right then to the left in the Northern Hemisphere. Thus the relative position and geometry of inner (point-bar) and outer (OBB) accumulations would vary

between successive bends. We expect that this asymmetry in deposition patterns between left and right bends will increase as a function of latitude, changing from a symmetric distribution at low latitudes to a highly asymmetric distribution at high-latitudes.

[14] **Acknowledgments.** R.C. was partially supported by the CGCS at the University of Toronto. M.G.W. acknowledges support from NSERC, CFI, and the Ontario MRI. The Metflow UDVP system was borrowed from Jeff Peakall of the NERC supported Sorby Environmental Fluid Dynamics Laboratory at Leeds University.

References

- Amos, K., J. Peakall, P. W. Bradbury, M. Roberts, G. Keevil, and S. Gupta (2010), The influence of bend amplitude and planform morphology on flow and sedimentation in submarine channels, *Mar. Pet. Geol.*, *27*, 1431–1447, doi:10.1016/j.marpetgeo.2010.05.004.
- Bruhn, C. H. L., and R. G. Walker (1997), Internal architecture and sedimentary evolution of coarse-grained, turbidite channel-levee complexes, Early Eocene Regencia Canyon, Espirito Santo Basin, Brazil, *Sedimentology*, *44*, 17–46, doi:10.1111/j.1365-3091.1997.tb00422.x.
- Carter, L., and R. M. Carter (1988), Late Quaternary development of left-bank-dominant levees in the Bounty trough, New Zealand, *Mar. Geol.*, *78*, 185–197, doi:10.1016/0025-3227(88)90108-9.
- Corney, R. K. T., J. Peakall, D. R. Parsons, L. Elliott, J. L. Best, R. E. Thomas, G. M. Keevil, D. B. Ingham, and K. J. Amos (2008), Reply to Discussion of Imran et al. on “The orientation of helical flow in curved channels” by Corney et al., *Sedimentology*, *53*, 249–257, *Sedimentology*, *55*(1), 241–247.
- Cossu, R., M. G. Wells, and A. K. Wahlin (2010), Influence of the Coriolis force on the velocity structure of gravity currents in straight submarine channel systems, *J. Geophys. Res.*, doi:10.1029/2010JC006208, in press.
- Imran, J., M. Islam, H. Huang, A. Kassem, C. Pirmez, J. Dickerson, and G. Parker (2007), Helical flow couplets in submarine gravity underflows, *Geology*, *35*, 659–662, doi:10.1130/G23780A.1.
- Islam, M. A., and J. Imran (2008), Experimental modeling of gravity underflow in a sinuous submerged channel, *J. Geophys. Res.*, *113*, C07041, doi:10.1029/2007JC004292.
- Johnson, G. C., and T. B. Sanford (1992), Secondary circulation in the Faoe bank channel outflow, *J. Phys. Oceanogr.*, *22*, 927–933, doi:10.1175/1520-0485(1992)022<0927:SCITFB>2.0.CO;2.
- Kane, I. A., W. D. McCaffrey, J. Peakall, and B. C. Kneller (2010), Submarine channel levee shape and sediment waves from physical experiments, *Sediment. Geol.*, *223*, 75–85, doi:10.1016/j.sedgeo.2009.11.001.
- Keevil, G. M., J. Peakall, J. L. Best, and K. J. Amos (2006), Flow structure in sinuous submarine channels: Velocity and turbulence structure of an experimental submarine channel, *Mar. Geol.*, *229*, 241–257, doi:10.1016/j.marpetgeo.2006.03.010.
- Klaucke, I., R. Hesse, and W. B. F. Ryan (1997), Flow parameters of turbidity currents in a low-sinuosity giant deep-sea channel, *Sedimentology*, *44*, 1093–1102.
- Komar, P. D. (1969), The channelized flow of turbidity currents with application to Monterey deep-sea fan channel, *J. Geophys. Res.*, *74*, 4544–4558, doi:10.1029/JC074i018p04544.
- Meiburg, E., and B. C. Kneller (2010), Turbidity currents and their deposits, *Annu. Rev. Fluid Mech.*, *42*, 135–156, doi:10.1146/annurev-fluid-121108-145618.
- Menard, H. W. (1955), Deep-Sea channels, topography, and sedimentation, *Am. Assoc. Pet. Geol. Bull.*, *39*, 236–255.
- Nakajima, T., J. Peakall, W. D. McCaffrey, D. A. Paton, and P. J. P. Thompson (2009), Outer-bank bars: A new intra-channel architectural element within sinuous submarine slope channels, *J. Sediment. Res.*, *79*, 872–886, doi:10.2110/jsr.2009.094.
- Nidzicko, N. J., J. L. Hench, and S. G. Monismith (2009), Lateral circulation in well-mixed and stratified estuarine flows with curvature, *J. Phys. Oceanogr.*, *39*(4), 831–851, doi:10.1175/2008JPO4017.1.
- Peakall, J., K. J. Amos, G. M. Keevil, P. W. Bradbury, and S. Gupta (2007), Flow processes and sedimentation in submarine channel bends, *Mar. Pet. Geol.*, *24*, 470–486, doi:10.1016/j.marpetgeo.2007.01.008.
- Pirmez, C., and J. Imran (2003), Reconstruction of turbidity currents in Amazon Channel, *Mar. Pet. Geol.*, *20*, 823–849, doi:10.1016/j.marpetgeo.2003.03.005.
- Straub, K. M., D. Straub, B. McElroy, J. Buttles, and C. Pirmez (2008), Interactions between turbidity currents and topography in aggrading sinuous submarine channels: A laboratory study, *Geol. Soc. Am. Bull.*, *120*, 368–385, doi:10.1130/B25983.1.

- Turner, J. S. (1973), *Buoyancy Effects in Fluids*, 367 pp., Cambridge Univ. Press, New York.
- Wählin, A. K. (2004), Downward channeling of dense water in topographic corrugations, *Deep Sea Res., Part I*, 51(4), 577–590.
- Wells, M. G. (2009), How Coriolis forces can limit the spatial extent of sediment deposition of a large-scale turbidity current, *Sediment. Geol.*, 218(1–4), 1–5, doi:10.1016/j.sedgeo.2009.04.011.
- Xu, J. P., M. A. Noble, and L. K. Rosenfeld (2004), In-situ measurements of velocity structure within turbidity currents, *Geophys. Res. Lett.*, 31, L09311, doi:10.1029/2004GL019718.

R. Cossu, Department of Geology, University of Toronto, 22 Russell St., Toronto, ON M5S 3B1, Canada. (remo.cossu@utoronto.ca)

M. G. Wells, Department of Physical and Environmental Sciences, University of Toronto, 1265 Military Trl., Toronto, ON M1C 1A4, Canada. (wells@utsc.utoronto.ca)